

# NUMERICAL STUDY OF INLET GAS VELOCITY EFFECTS ON DROPLET BEHAVIORS IN MICROCHANNEL

Mengcheng Jiang, Biao Zhou<sup>1</sup>

Department of Mechanical, Automotive and Materials Engineering  
University of Windsor  
Windsor, ON, Canada, N9B 3P4

**Abstract**—In this study, the numerical simulation of liquid water behaviors inside a single straight microchannel is conducted using Volume of fluid (VOF) method and dynamic contact angle (DCA) model. Two different gas inlet velocities are considered in the simulation to investigate the gas velocity effects on the droplet behaviors. The general process of the liquid water evolvment inside the channel are presented and discussed. The results indicate that the water droplet will form into long slug flow under lower gas inlet velocity and thin film flow under higher gas inlet velocity.

**Keywords**—droplet behaviors; microchannel; volume of fluid method; dynamic contact angle.

## I. INTRODUCTION

Proton exchange membrane fuel cells (PEMFCs) are energy conversion devices that can produce electrical power from hydrogen and air, releasing only water and heat. PEMFC is one of the promising energy power sources for next-generation vehicles and distributed power applications, mainly because of their advantages such as zero-emission, low operation temperature, high power density and quietness.

However, water management is still one of the most critical challenges for fuel cell commercialization. Thoroughly understanding the gas-liquid dynamics inside PEMFCs will help researchers to optimize the PEMFC designs. Numerical simulation using volume of fluid (VOF) method has been recognized as an effective approach to investigate the liquid water behaviors inside the gas channels. So far, for PEMFC-related simulations, the static contact angle (SCA) model is generally used [1-7] while the dynamic contact angle (DCA) model is still under development. Recently, several researchers have applied DCA model to simulate the droplet dynamics and evolvment [8-11] and it is indicated that DCA model is more applicable than SCA model in the prediction of droplet behaviors. Zhou's group proposed the AR-DCA model [12] implemented with Hoffman function [13], which is able to simulate both advancing and receding dynamic contact angles. This AR-DCA model has been successfully validated against a series of experiments for droplet impact on horizontal and inclined surfaces from Sikalo et al. [14, 15], showing its potential to be applied in the simulation of gas-liquid two-phase in microchannels.

However, only a few of the researchers reported the simulations of droplet behaviors in microchannels using DCA model: Fang et al. [16] employed a contact angle hysteresis model to simulate gas-liquid flows and the results showed that the contact angle distribution in the microchannel will significantly affect the slug elongation and instability; Miller [17] and Wu [18] implemented DCA model with Hoffman function to simulate the liquid water transport and behaviors in gas channel, and it is indicated that the dynamic contact line treatment is very crucial in the simulation of gas-liquid dynamics.

In this study, as one part of the progress for the DCA model development, we further extend our research to the simulation of droplet behaviors in a single straight microchannel. The numerical results under different gas inlet velocity will be presented and discussed.

## II. NUMERICAL MODEL DESCRIPTION

### A. Computational Domain

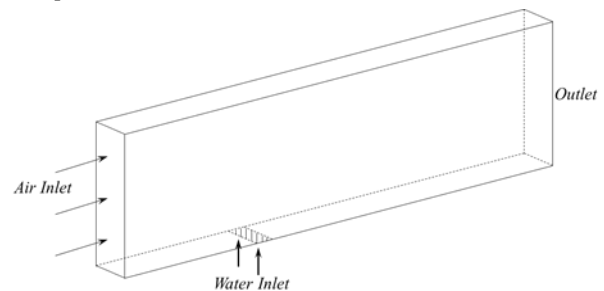


Figure 1. Schematic of computational domain in this study.

In this study, a three-dimensional single straight channel with rectangular cross section is built up as the computational domain. The dimensions of the channel are 0.05 mm in depth, 0.5 mm in width and 5 mm in length. The liquid water enters into the channel through a 0.02 mm rectangular slot on the bottom wall, which is located at 1.65 mm away from the inlet boundary.

### B. Computational Methodology

In the simulation, the VOF method is used to track the gas-liquid flow interface. The governing equations are as follows:

<sup>1</sup> Corresponding Author and Principal Investigator: Dr. Biao Zhou, [bzhou@uwindsor.ca](mailto:bzhou@uwindsor.ca), 1-519-253-3000 ext. 2630

The mass conservation equation:

$$\frac{\partial(\rho)}{\partial t} + \nabla \cdot (\rho \vec{u}) = 0 \quad (1)$$

The mixture density and viscosity in each computational cell can be calculated by:

$$\rho = s_l \rho_l + s_g \rho_g \quad (2)$$

$$\mu = s_l \mu_l + s_g \mu_g \quad (3)$$

where  $s_l$  and  $s_g$  are the liquid and gas volume fraction respectively, and the sum of the volume fraction is:

$$s_l + s_g = 1 \quad (4)$$

Then the continuity equation for the liquid phase can be expressed as the following form:

$$\frac{\partial(s_l \rho_l)}{\partial t} + \nabla \cdot (s_l \rho_l \vec{u}) = 0 \quad (5)$$

The momentum equation is:

$$\frac{\partial}{\partial t} (\rho \vec{u}) + \nabla \cdot (\rho \vec{u} \vec{u}) = -\nabla p + \nabla \cdot [\mu (\nabla \vec{u} + \nabla \vec{u}^T)] + S_m \quad (6)$$

The surface normal  $\hat{n}$  is determined by:

$$\hat{n} = \hat{n}_w \cos \theta_d + \hat{t}_w \sin \theta_d \quad (7)$$

where  $\hat{n}_w$  and  $\hat{t}_w$  represent the unit vectors normal and tangential to the wall respectively. Dynamic contact angle  $\theta_d$  is applied at the wall boundaries through a user defined function (UDF) code. The methodology to calculate and implement  $\theta_d$  has been reported in our previous work [12] and more details can be found in [12].

### C. Boundary Conditions and Mesh Set Up

In the numerical simulation, the no-slip boundary condition is applied at channel walls. The DCA is considered on both side wall and bottom wall. The initial contact angle (i.e., SCA) for all the boundary walls is  $108^\circ$ . The volume flow rate of liquid water is set as  $50 \mu\text{L}/\text{min}$ ; the gas inlet velocities  $V_{inlet}$  are set as  $4.8 \text{ m/s}$  and  $21.9 \text{ m/s}$  respectively to investigate the effects of different gas inlet velocities on the droplet behaviors and evolution.

The whole computational domain is meshed by approximately 125500 cells, with minimum cell volume of  $2 \times 10^{-7} \text{ mm}^3$  and maximum cell volume of  $1.4 \times 10^{-6} \text{ mm}^3$ . The grid size is approximately  $0.01 \text{ mm}$  in X-, Y- and Z- direction with a grid refinement applied near the bottom wall.

## III. RESULTS AND DISCUSSION

Fig. 2 presents the water droplet evolution process in the single straight microchannel under relative low velocity ( $V_{inlet} = 4.8 \text{ m/s}$ ), with the liquid water volume fraction contours. The dark blue area represents the gas phase while the red area represents the liquid water. From this series of figure under selected time instances, the main process of droplet evolution can be described as follows:

- 1) At the very beginning, the water enters into the channel with a constant volume flow rate, as shown in Fig. 2(a).
- 2) The liquid water continues to emerge and form the droplet with time (from  $t = 0.2 \text{ ms}$  to  $10 \text{ ms}$ , as shown in Fig. 2(b-c)).
- 3) When it comes to about  $16.4 \text{ ms}$ , the droplet almost blocks the channel (Fig. 2(d)) and reaches a critical point; then the droplet is blown away towards the outlet direction due to the force exerted at the windward side from the inlet gas, as shown in Fig. 2(e).
- 4) From  $t = 16.6 \text{ ms}$  to  $18.0 \text{ ms}$  (Fig. 2(e-g)), the droplet significantly deforms from “tall-standing” shaped slug to “long-lying” shaped slug, mainly due to the continuous pressure from the inlet gas and the interactions among the pressure, surface tension and shear stress.
- 5) After  $18.0 \text{ ms}$ , the deformation and evolution of the water slug become stable, as shown in Fig. 2(g-h).

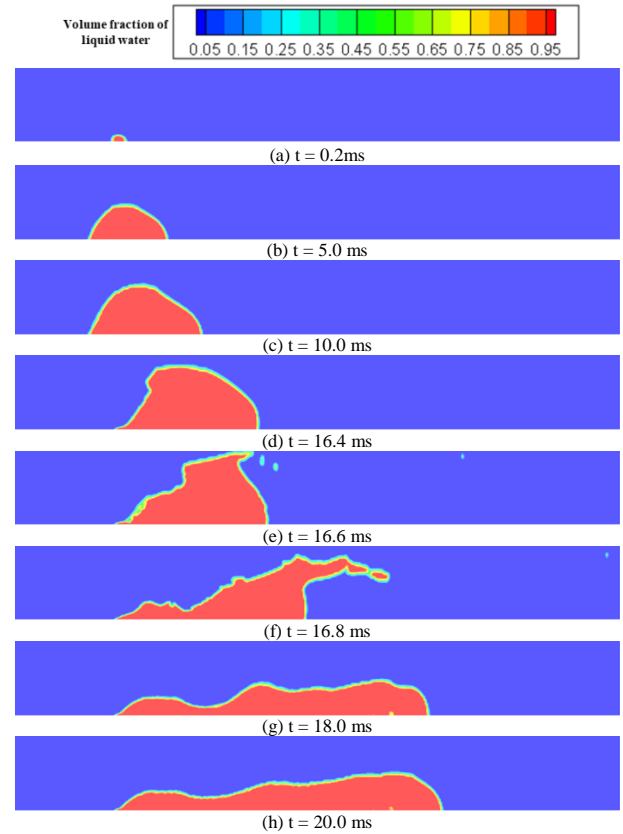


Figure 2. Liquid water droplet evolution under  $V_{inlet} = 4.8 \text{ m/s}$ .

When the air inlet velocity is increased to  $21.9 \text{ m/s}$ , the remarkably different phenomena for the droplet behaviors and evolution can be observed, as shown in Fig. 3.

- 1) At the beginning of the simulation, the water enters into the channel with a constant volume flow rate, as shown in Fig. 3(a).

- 2) From  $t = 2.0$  ms to 4.4 ms, the droplet continues to grow in the microchannel. Due to the higher gas inlet velocity, the droplet starts to deform at the early stage and tends to form small liquid film at the trailing side, as shown in Fig. 3(c).
- 3) From  $t = 4.4$  ms, when the deformation reaches a critical point, the upper part of the droplet is blown away, as shown in Fig. 3(d-e).
- 4) After 4.6 ms, the water droplet deforms into film flow and moves along the bottom wall. Some small splashed water droplet can also be observed in the channel, as shown in Fig. 3(f). This is mainly caused by the high pressure and strong air flow between the upper wall and the top side of droplet.
- 5) With time, the water accumulates at the leading side and forms a new droplet, as shown in Fig. 3(g), and the rest remains in the regime of film flow.
- 6) As shown in Fig. 3(h), the droplet further elongates and forms a long, thin and continuous film flow with waves. The liquid water will also drain out through the outlet.

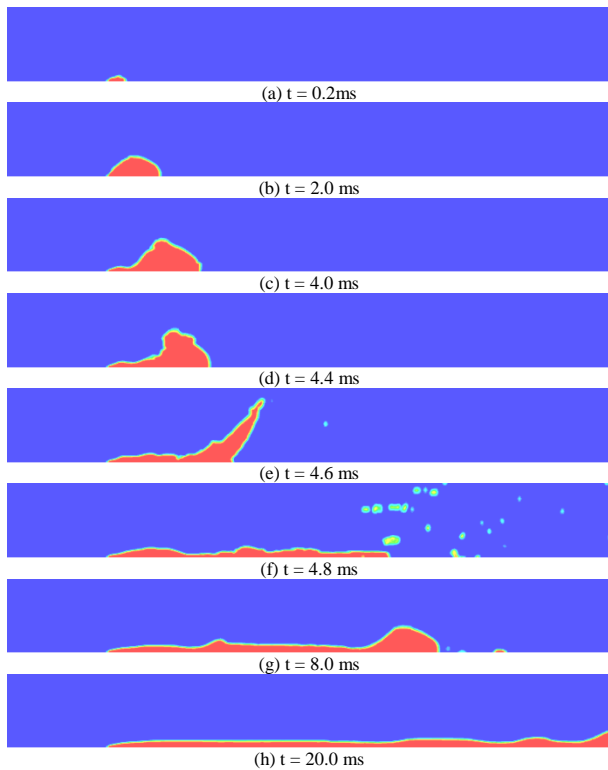


Figure 3. Liquid water droplet evolution under  $V_{inlet} = 21.9$  m/s.

#### IV. CONCLUSIONS

This paper presents the numerical study of droplet behavior and evolution in a single straight microchannel. The effects of gas inlet velocity are investigated by considering two different conditions (4.8 m/s and 21.9 m/s).

Dynamic contact angle is considered as one of the wall boundary conditions instead of static contact angle.

From the numerical results, it can be found that the two cases in this study (one with lower gas inlet velocity and another with higher velocity) share some similar droplet evolution phenomena: the droplet first emerge and grow inside the channel near the liquid inlet area; with time, the droplet will reach a critical point and then be blown away towards the channel outlet side.

Also, several significantly different phenomena can also be captured: under lower gas inlet velocity (4.8 m/s), the liquid water can remain in a droplet much longer than that of the higher inlet velocity condition (21.9 m/s); within the same time period (20 ms), the liquid water will form into long slug flow under lower inlet velocity, while the continuous long film flow can be observed under higher inlet velocity. It can be concluded that the gas inlet velocity has remarkable effects on the droplet deformation and evolution in the microchannel, mainly reflected in the flow regime.

#### ACKNOWLEDGMENT

The authors are grateful for the support from the Natural Sciences and Engineering Research Council of Canada (NSERC) and the University of Windsor. The authors also would like to thank Compute Canada and Sharcnet for the support of computing resource.

#### REFERENCES

- [1] Jiao K, Zhou B. Accelerated numerical test of liquid behavior across gas diffusion layer in proton exchange membrane fuel cell cathode. *Journal of Fuel Cell Science and Technology*. 2008 Nov 1;5(4):041011.
- [2] Le AD, Zhou B. Fundamental understanding of liquid water effects on the performance of a PEMFC with serpentine-parallel channels. *Electrochimica Acta*. 2009 Mar 1;54(8):2137-54.
- [3] Kang S, Zhou B, Cheng CH, Shiu HR, Lee CI. Liquid water flooding in a proton exchange membrane fuel cell cathode with an interdigitated design. *International Journal of Energy Research*. 2011 Dec 1;35(15):1292-311.
- [4] Wang X, Zhou B. Liquid water flooding process in proton exchange membrane fuel cell cathode with straight parallel channels and porous layer. *Journal of Power Sources*. 2011 Feb 15;196(4):1776-94.
- [5] Ding Y, Bi XT, Wilkinson DP. Numerical investigation of the impact of two-phase flow maldistribution on PEM fuel cell performance. *International Journal of Hydrogen Energy*. 2014 Jan 2;39(1):469-80.
- [6] Ashrafi M, Shams M, Bozorgnezhad A, Ahmadi G. Simulation and experimental validation of droplet dynamics in microchannels of PEM fuel cells. *Heat and Mass Transfer*. 2016 Dec 1;52(12):2671-86.
- [7] Ferreira RB, Falcão DS, Oliveira VB, Pinto AM. 1D+ 3D two-phase flow numerical model of a proton exchange membrane fuel cell. *Applied Energy*. 2017 Oct 1;203:474-95.
- [8] Šikalo Š, Wilhelm HD, Roisman IV, Jakirlić S, Tropea C. Dynamic contact angle of spreading droplets: Experiments and simulations. *Physics of Fluids*. 2005 Jun;17(6):062103.
- [9] Lunkad SF, Buwa VV, Nigam KD. Numerical simulations of drop impact and spreading on horizontal and inclined surfaces. *Chemical Engineering Science*. 2007 Dec 31;62(24):7214-24.
- [10] Legendre D, Maglio M. Numerical simulation of spreading drops. *Colloids and Surfaces A: Physicochemical and Engineering Aspects*. 2013 Sep 5;432:29-37.
- [11] Jiang M, Zhou B. Numerical study of droplet impact on inclined surface: viscosity effects. *ECS Transactions*. 2018 Jan 4;83(1):127-36.

- [12] Jiang M, Zhou B, Wang X. Comparisons and validations of contact angle models. *International Journal of Hydrogen Energy*. 2018 Mar 2.
- [13] Kistler SF. Hydrodynamics of wetting. *Wettability*. 1993;6:311-430.
- [14] Šikalo Š, Tropea C, Ganić EN. Impact of droplets onto inclined surfaces. *Journal of Colloid and Interface Science*. 2005 Jun 15;286(2):661-9.
- [15] Šikalo Š, Ganić EN. Phenomena of droplet–surface interactions. *Experimental Thermal and Fluid Science*. 2006 Nov 30;31(2):97-110.
- [16] Fang C, Hidrovo C, Wang FM, Eaton J, Goodson K. 3-D numerical simulation of contact angle hysteresis for microscale two phase flow. *International Journal of Multiphase Flow*. 2008 Jul 31;34(7):690-705.
- [17] Miller C. Liquid water dynamics in a model polymer electrolyte fuel cell flow channel, MSc Thesis, University of Victoria, 2009.
- [18] Wu TC. Two-phase flow in microchannels with application to PEM fuel cells, PhD Dissertation, University of Victoria, 2015